

MR angiography-planned prostatic artery embolization for benign prostatic hyperplasia: single-center retrospective study in 56 patients

Thomas J. Vogl 
Annette Zinn 
Elsayed Elhawash 
Leona S. Alizadeh 
Nour-Eldin A. Nour-Eldin 
Nagy N. N. Naguib 

PURPOSE

We aimed to evaluate the advantages of magnetic resonance angiography (MRA)-planned prostatic artery embolization (PAE) for benign prostatic hyperplasia (BPH).

METHODS

In this retrospective study, MRAs of 56 patients (mean age, 67.23±7.73 years; age range, 47–82 years) who underwent PAE between 2017 and 2018 were evaluated. For inclusion, full information about procedure time and radiation values must have been available. To identify prostatic artery (PA) origin, three-dimensional MRA reconstruction with maximum intensity projection was conducted in every patient. In total, 33 patients completed clinical and imaging follow-up and were included in clinical evaluation.

RESULTS

There were 131 PAs with a second PA in 19 pelvic sides. PA origin was correctly identified via MRA in 108 of 131 PAs (82.44%). In patients in which MRA allowed a PA analysis, a significant reduction of the fluoroscopy time (-27.0%, $p = 0.028$) and of the dose area product (-38.0%, $p = 0.003$) was detected versus those with no PA analysis prior to PAE. Intervention time was reduced by 13.2%, ($p = 0.25$). Mean fluoroscopy time was 30.1 min, mean dose area product 27,749 $\mu\text{Gy}\cdot\text{m}^2$, and mean entrance dose 1553 mGy. Technical success was achieved in all 56 patients (100.0%); all patients were embolized on both pelvic sides. The evaluated data documented a significant reduction in international prostate symptom scores ($p < 0.001$; mean 9.67 points).

CONCLUSION

MRA prior to PAE allowed the identification of PA in 82.44% of the cases. MRA-planned PAE is an effective treatment for patients with BPH.

A profound knowledge about pelvic vessel anatomy is essential for achieving successful prostatic artery embolization (PAE), to improve the safety of PAE and to avoid major complications as non-target embolization (1–6). This knowledge can be achieved by using angiographic techniques to show pelvic artery anatomy, although the best method is still controversially discussed. In some studies, computed tomography (CT) angiography (CTA) was used for pre-interventional evaluation as it is described to have high certainty in analyzing prostatic artery (PA) anatomy (1, 3, 7). Other institutes use digital subtraction angiography (DSA) and cone beam CT (CBCT) for analysis without any pre-procedural vessel imaging (8–11). Since peri-interventional DSA findings may be ambiguous and CTA or CBCT would imply additional radiation, magnetic resonance angiography (MRA) seems to be a promising method to analyze PA origin without radiation. However, Maclean et al. (3) recommend CT for planning PAE instead of magnetic resonance imaging (MRI) as the latter is more expensive and more time-consuming. Pisco et al. (5, 12) state that MRA does not have enough resolution for clear identification of PA origin and does not provide the same information as CTA.

Currently only a few studies discuss the suitability of MRA for preprocedural planning of PAE. Kim et al. (13) first investigated this subject with a sample size of 17 patients and documented an accuracy of 76.5% for PA origin analysis. However, in this study no clinical evaluation was included. Zhang et al. (4) investigated MRA analysis prior to PAE in a randomized

From Institute of Diagnostic and Interventional Radiology (T.J.V. ✉ T.Vogl@em.uni-frankfurt.de, A.Z., E.E., L.S.A., N.A.N.), University Hospital Frankfurt, Frankfurt, Germany; Department of Diagnostic and Interventional Radiology (N.A.N.), Cairo University Hospital, Cairo, Egypt; Department of Radiology (N.N.N.N.), AMEOS Hospital Halberstadt, Halberstadt, Germany; Department of Diagnostic and Interventional Radiology (N.N.N.N.), Alexandria University Hospital, Alexandria, Egypt.

Received 24 March 2020; revision requested 25 May 2020; last revision received 17 September 2020; accepted 8 October 2020.

Published online 21 September 2021.

DOI 10.5152/dir.2021.20124

You may cite this article as: Vogl TJ, Zinn A, Elhawash E, et al. MR angiography-planned prostatic artery embolization for benign prostatic hyperplasia: single-center retrospective study in 56 patients. *Diagn Interv Radiol* 2021; 27:725–731.

clinical trial with 100 patients. A sensitivity of 91.5% and a significant reduction of procedure time, fluoroscopy time, radiation dose, and contrast medium volume due to pre-interventional MRA were documented. In his review, Prince (14) agrees with Zhang et al. (4) that MRA may be a suitable method for planning PAE.

Because of the skeptical comments whether performing MRA prior to PAE is practical on a daily basis in a radiological institution, an assessment of these parameters in a less selective nature was necessary. In addition, contrary to Zhang et al. (4) who used MIP-reconstructions and 5° interval images for their assessment, we used a three-dimensional (3D) reconstruction of the pelvic arterial tree based on the MRA sequences. The main advantage of the 3D reconstruction is that it can be freely rotated in all directions which allowed an easy identification and tracking of the PA.

In this study, the advantages and clinical outcome of pre-interventional analysis of PA via MRA as a possible radiation-free planning method and its influence on procedure time and radiation dose were investigated.

Methods

Study population

This retrospective single-center study was approved by the ethical committee and all patients signed an informed consent before MRA and PAE.

Between January 2017 and April 2018, PAE was performed in 60 patients at our institute. MRA was performed within 2 weeks before the procedure of PAE. For inclusion, the patients needed a pre-interventional MRA at our institute as well as a complete dataset concerning duration of procedure and radiation values. One patient did not receive MRA before PAE and in 3 patients no detailed intervention time was documented. Therefore, 56 patients were included in

Main points

- MRA provided correct analysis of prostatic artery (PA) origin in 82.4% of cases.
- The most common origin of the PA is the internal pudendal artery.
- Successful analysis of PA origin significantly reduces fluoroscopy time and radiation dose.
- MRA-planned PA embolization has a clinical success rate of 72.7%.

Table 1. Baseline values of the patients before prostatic artery embolization

Value	Measurements n=56
Age (years), mean±SD (min–max)	67.23±7.73 (47–82)
PV (mL), mean±SD (min–max)	85.63±54.1 (35.3–310.6)
IPSS, n (%)	43 (76.8%)
IPSS, mean±SD (min–max)	21.7±6.77 (11–35)
QoL, n (%)	43 (76.8%)
QoL, mean±SD (min–max)	4.05±1.36 (0–6)
IIEF, n (%)	43 (76.8%)
IIEF, mean±SD (min–max)	17.6±10.05 (1–30)

SD, standard deviation; PV, prostate volume; IPSS, international prostate symptom score (possible range, 0–35); QoL, quality of life score (possible range, 0–6); IIEF, international index of erectile function (possible range, 1–30).

data evaluation. Overall, 44 patients had MRI follow-up and 40 patients filled in the clinical questionnaires comprising International Prostate Symptom Score (IPSS), Quality of Life (QoL) score and International Index of Erectile Function (IIEF) before and after PAE as a part of the quality management. In total, 33 patients completed both clinical and imaging follow-up and were included in the clinical outcome evaluation. The majority of the patients had MRI follow-up after 4.2 months. Clinical follow-up was extended up to 12 months due to the retrospective study design since not all patients filled in the questionnaire at a defined point of time.

The baseline characteristics of the patients including age, prostate volume (PV), IPSS, QoL and IIEF are listed in Table 1.

Prostatic artery embolization

All PAE procedures were performed on a single angiography unit (Artis Pheno, Siemens Healthineers) by two interventional radiologists with over 15 and 30 years of experience. All patients obtained written informed consent for this procedure. After injecting local anesthesia (Mecain 10 mg/mL; PUREN Pharma GmbH & Co. KG), a unilateral transfemoral approach was used for catheterization of the pelvic arteries. First a crossover maneuver was performed to access the contralateral common iliac artery using a 5 F Pig-Tail catheter (Boston Scientific). This was followed by selective catheterization of the internal iliac artery using a 5 F Side-Winder catheter (Terumo) which was later exchanged for a 4 F Cobra C2 hydrophilic catheter (Terumo). Superselective catheterization of the prostatic artery was performed using a 2.0 F Microcatheter in all cases (Progreat 2 F, Terumo). The tip of the

microcatheter was advanced deep in the inferior vesical artery, distal to all collaterals supplying the bladder, rectum and penis, to prevent embolization of possible anastomoses. In case of any collaterals selective embolization of the collateral vessel was performed using microcoils before injecting the embolizing material. For all patients the embolization was performed using 300–500 µm Embospheres (Merit Medical) until stasis was observed. This was followed by embolization of the ipsilateral side.

In a few number of cases CBCT was performed for identification of the PA and in case of uncertainty regarding potential anastomoses with other important branches of the internal iliac artery. In total, 14 CBCTs were conducted in seven patients. No patient included in this study needed protective coils.

MRI

Before PAE, an initial MRI and contrast-enhanced MRA were performed as a part of the pre-interventional examination. Imaging was performed with a 3.0 T MRI system (MAGNETOM Prisma; Siemens Healthineers) and a body array coil. Gradient-echo scout images (repetition time/echo time [TR/TE], 6.9/3.75 ms; flip angle, 35°; section thickness, 8 mm; matrix, 192×256; field of view [FOV], 45 cm) as well as T2-weighted single-shot turbo spin-echo images (TR/TE 7500/100 ms; flip angle, 160°; section thickness, 3.5 mm; matrix, 320×320; voxel dimensions, 0.6×0.6×3.5 mm; FOV, 20 cm) were performed in the axial, coronal, and sagittal direction.

An unenhanced 3D fast low-angle shot sequence (TR/TE, 3.1/1.12 ms; flip angle, 30°; section thickness, 0.9 mm; matrix, 312×416; FOV, 38 cm; voxel dimensions,

0.9×0.9×0.9 mm) was obtained before conducting the contrast-enhanced MRA with a 3D fast low-angle shot sequence (TR/TE 3.1/1.12 ms; flip angle, 30°; section thickness, 0.9 mm; matrix, 312×416; FOV, 38 cm; voxel dimensions, 0.9×0.9×0.9 mm) in the arterial and venous phases. For determining contrast medium flow time, a test bolus was applied. Between 7 to 12 mL of gadolinium-based contrast media (Gadovist 1.0 mmol/L, Bayer Vital GmbH) were injected at a rate of 2 mL/s. No nitroglycerine was used prior to the contrast media.

Image reconstruction and image evaluation

Subtracted images were used to create maximum-intensity projection (MIP) reconstructions and a 3D freely rotatable, volume-rendered model of pelvic arteries at our workstation (syngo.via[®]; Siemens Healthineers). 3D reconstruction was used to examine the potentially best C-arm oblique angle and to visualize PA origin and its course (Fig.).

Raw contrast-enhanced images, MIP and 3D reconstructions were used all together to analyze origin, trajectory, and numbers of PA. PA was identified due to its course, target and corkscrew pattern if existent (1, 6). All MRA images were reconstructed and analyzed by two radiologists, with over 7 and 15 years of experience, in consensus. Neither of the two radiologists had access to the angiographic images at the time of evaluation.

The classification used to categorize PA origins was introduced by Assis et al. (2) in 2015. Therefore, PA origin was classified in five groups: from the anterior division of the internal iliac artery together with the superior vesical artery (type I), from the anterior division of the internal iliac artery inferior to the superior vesical artery (type II), from the obturator artery (type III), from the internal pudendal artery (type IV), or from less common origins including a trifurcation or quadrifurcation of the anterior division of the inferior gluteal artery and branches of the external iliac artery (type V). The analyzed PA origin was documented separately for MRA and retrospectively compared to DSA findings as the gold standard to provide the sensitivity.

Initial and post-embolization volumetry was performed via analysis of axial and sagittal T2-weighted sequences and calculated with axial, anterior-posterior and cranio-caudal diameter (height×width×length × 0.52).

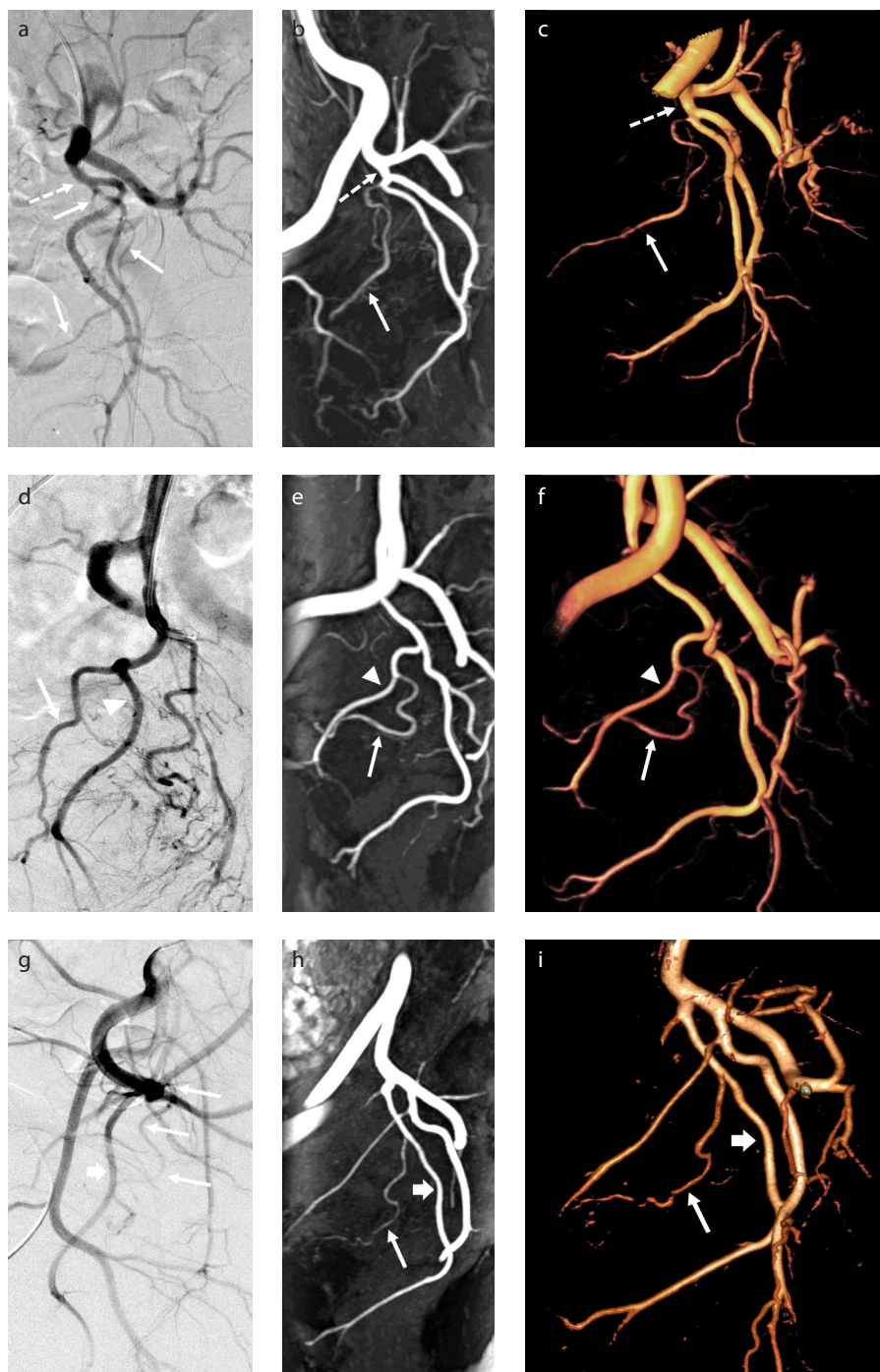


Figure. a–i. MIP and three-dimensional (3D) reconstruction of MRA. DSA (a), MIP (b) and 3D reconstruction (c) of a prostatic artery (PA; plain arrow) arising from the common gluteal-pudendal trunk (dotted arrow) together with the superior vesical artery, classified as type I. DSA (d), MIP (e) and 3D reconstruction (f) of a PA origin from the obturator artery (arrowhead), classified as type III. DSA (g), MIP (h) and 3D reconstruction (i) of PA originating from the internal pudendal artery (bold arrow), classified as type IV.

Data collection

All data were extracted from the clinical database. During the procedure intervention time, which stands for the room time, fluoroscopy time, dose area product (DAP) and entrance dose were recorded. Clinical improvement and success were assessed

via IPSS and QoL. IIEF data were collected for detecting complications, namely erectile dysfunction. PV data were collected to evaluate the effects of PAE on morphologic aspects.

Table 2 presents a comparison between the groups with successful and non-suc-

Table 2. Comparison of patients with PA visible on MRA (Group 1) and those with PA not visible on MRA (Group 2)

	Group 1	Group 2	<i>p</i>
Total pelvic sides	92	20	
Age (years)	66.53±7.58 (47–82)	70.45±7.57 (59–80)	0.064
PV (mL)	89.12±57.02 (36.28–310.56)	69.54±32.28 (35.33–119.02)	0.13
Atherosclerosis	0.47±0.58 (0–2)	0.45±0.6 (0–1)	0.90
Vessel tortuosity	1.53±0.87 (0–4)	1.55±0.89 (0–3)	0.92

Data are presented as mean±standard deviation (min–max). PA, prostatic artery; MRA, magnetic resonance angiography; PV, prostate volume.

Table 3. Results of the analysis of the prostatic artery origin from each pelvic side and their distribution over types I–V

n=131		n (%)
Origin successfully detected in MRA		108 (82.44)
No origin or failed detection in MRA		23 (17.56)
Type	Vessel of origin	
I	Anterior division together with superior vesical artery	21 (19.44)
II	Anterior division below superior vesical artery	5 (4.63)
III	Obturator artery	12 (11.11)
IV	Internal pudendal artery	55 (50.93)
V	Rare origins	15 (13.89)
	- Inferior gluteal artery	3 (2.78)
	- External iliac artery	1 (0.93)
	- Trifurcation or quadrifurcation of anterior division	11 (10.19)

MRA, magnetic resonance angiography.

Table 4. Procedural time and fluoroscopy measurements during the prostatic artery embolization

n=56	Mean±SD	Min–max
Intervention time (min)	86.3±34.0	32–168
Fluoroscopy time (min)	30.1±15.3	5.0–68.7
Image and fluoroscopy dose area product (μGy·m ²)	27,749±22,900	2925–135,640
Entrance dose (mGy)	1553±1183.13	110–6437

SD, standard deviation.

Successful PA analysis via MRA. Characteristics of the patients which might interfere with the quality of MRA are listed. Therefore, differences in mean age, PV, level of atherosclerosis and level of vessel tortuosity between the groups were assessed. Level of atherosclerosis was categorized in three groups with 0 denoting no signs of atherosclerosis, 1 denoting moderate irregularities of the vessels, and 2 denoting high-grade stenosis over 50% in the aorta, internal and external iliac artery in DSA. Level of vessel tortuosity was evaluated through the number of turns of the iliac artery and its branches in DSA images until reaching the origin of PA.

Technical success was characterized as successful selective catheterization of the target vessel and successful uni- or bilateral embolization of the prostate-supplying arteries. Clinical success was determined by IPSS-reduction of ≥25% and post-procedural IPSS ≤ 17 points as well as QoL score reduction of ≥1 point or post-procedural QoL score ≤3 points (12, 15).

Statistical analysis

Statistical analyses were performed using Microsoft® Excel® for Office 365 (MSO 32. Bit, version 1808 (16.0.10730.20102), © 2018 Microsoft Corporation) and BiAS for

Windows (version 11.08-03/2018, © Epsilon Verlag 1989-2018). Normality of data distribution was evaluated for all variables via Kolmogorov-Smirnov-Lilliefors test. Paired t-test for IPSS and Wilcoxon matched pairs test for QoL, IIEF and PV were applied in order to assess the significance of changes before and after PAE. For group comparison Wilcoxon-Mann-Whitney U test was used. Difference of procedure time, fluoroscopy time, dose area product (DAP) and entrance dose was calculated as differences between the means of both groups. A *p* value < 0.05 was considered to be significant. The comparison was made between MRA-planned PAE and DSA-guided PAE.

Results

The MRA analysis showed 111 of 131 PAs in 112 pelvic sides of 56 patients (patients had a mean age of 67.23±7.73 years, range 47–82 years). In three pelvic sides, PA origin was analyzed incorrectly, while in 108 PAs correct analysis was confirmed via the gold standard DSA. Therefore, MRA allowed the correct analysis of PA origin in 108 of 131 PAs (82.44%) (Table 3).

Overall, 55 PAs (50.93%) originated from the internal pudendal artery, whereas 21 PAs (19.44%) originated from the anterior division of internal iliac artery in a common trunk with the superior vesical artery and 5 (4.63%) inferior to the superior vesical artery. In 12 cases (11.11%) obturator artery and in 15 cases (13.89%) less common vessels were determined as PA origin. One PA arose from a branch of the external iliac artery (0.93%), 3 PAs from the inferior gluteal artery (2.78%) and 11 PAs (10.19%) from a trifurcation or quadrifurcation of anterior division. In 19 pelvic sides, a second PA was seen. All of those originated from the internal pudendal artery except one artery arising from the inferior gluteal artery. In 20 pelvic sides, no PA was seen in MRA, but the artery and its origin was identified via DSA during PAE procedure. In 7 patients neither the left nor the right PA origin was visible, whereas in 6 patients only one pelvic side was analyzed with certainty.

No significant difference in mean age (*p* = 0.064), PV (*p* = 0.13), level of atherosclerosis (*p* = 0.90) and level of vessel tortuosity (*p* = 0.92) were found between the groups with successful PA analysis and non-successful analysis (Table 2).

Mean intervention time was 86.3 minutes, mean time of fluoroscopy 30.1 min-

utes, mean DAP was 27,749 μGym^2 , and mean entrance dose was 1553 mGy (Table 4). The group with successful MRA had a significantly lower fluoroscopy time ($p = 0.028$), DAP ($p = 0.003$) and entrance dose ($p = 0.003$) (Table 5). Patients with successful MRA prior to PAE on one or both sides had a 13.2% shorter procedure time, 27.0% shorter fluoroscopy time, 38.0% lower DAP and 37.1% lower entrance dose than patients with no successful PA analysis before PAE.

Technical success was achieved in all 56 patients (100.0%). All patients were embolized on both pelvic sides. Clinical success was registered in 24 of 33 patients with completed clinical and imaging follow-up (72.7%). Detailed changes in all evaluated variables before and after PAE are listed in Table 6.

A significant improvement of IPSS ($p < 0.001$) was found with a mean change of -9.67 ± 8.21 points (range -30 to +8 points; 95% CI: -12.58 to -6.75) which equals $-45.58\% \pm 31.88\%$ (range, -88.0% to +30.0%; 95% CI: -56.81% to -34.24%) along with a significant increase in QoL ($p < 0.001$) with -1.63 ± 1.45 points (95% CI: -2.15 to -1.12) with a range of -4 up to +2 points (-41.70% $\pm 36.36\%$, range -100% to +50%; 95% CI: -54.59% to -28.80%) and significant increase in IIEF ($p = 0.004$; mean $+2.88 \pm 6.14$

points, range -8 to +26 points; 95% CI: 0.70 to 5.06).

PAE significantly reduced PV ($p < 0.001$). Mean percent reduction was $9.03\% \pm 12.96\%$ with a range of -50.1% up to +17.7% (95% CI: -13.63% to -4.44%) which equals -6.91 ± 9.46 mL with a range of -38.15 mL up to +7.47 mL (95% CI: -10.26 to -3.55).

In the observed period of time, only a few minor adverse events and no major adverse events occurred. Transient hematuria was observed in 8 patients. In 4 patients, a transient urinary infection or prostatitis was documented. Six patients endured postembolization pain, which in 3 cases persisted for more than 7 days. None of the complications required hospitalization; all were managed conservatively and occurred only for a short period of time.

Discussion

This study evaluates the advantages of pre-interventional MRA for analyzing the prostatic artery and its influence on procedure time and radiation dose, as well as the efficacy of the MRA-planned PAE in order to treat benign prostate hyperplasia.

Successful PA analysis via MRA prior to the procedure significantly reduces fluoroscopy time and radiation dose. As older age, increased vessel tortuosity and atherosclerosis can be associated with poor angio-

graphic results as well as increased procedure and fluoroscopy time, a comparison of the groups with and without successful MRA concerning these factors was required (16). In our analysis, both groups showed a similar profile concerning age, PV, atherosclerosis, and vessel tortuosity. Although both groups seem to have similar demographics, those factors might still have an impact on image quality. Nevertheless, reduced fluoroscopy time and radiation dose seems to be a result of preprocedural planning.

Therefore, there must be further reasons why MRA failed in this group of patients. In 5 patients with no origin visible on either side, venous vessels were contrasted; in the other two patients, the available field of view was too small to show all relevant pelvic arteries. Further reasons for failure of MRA analysis besides poor timing of contrast and incomplete visualization of the pelvic artery anatomy can be slow application of the contrast bolus, inadequate volume of contrast media, artifacts because of patient movement or a small vessel diameter (< 0.5 mm) (4, 13). Although a high spatial resolution (matrix, 312×416) and thin sections (0.9 mm) were used for visualization in this study, the technical quality of MRA as well as reconstruction quality is user dependent.

Reconstructed MRA allowed the detection of the prostate supplying artery and its origin with a sensitivity of 82.44%, which lies between findings from the two previous studies investigating MRA prior to PAE.

In their retrospective pilot study with 17 patients, Kim et al. (13) detected an accuracy of 76.5% in comparison to the origin of PA seen in peri-procedural DSA. A PA-origin was seen in 31 of 34 pelvic sides and 27 of them were analyzed correctly. No information about baseline parameters,

Table 5. Comparison of the evaluated measurements between the two MRA groups

	Procedure time (min)	Fluoroscopy time (min)	DAP (μGym^2)	Entrance dose (mGy)	IPSS reduction (%)
PA origin seen on MRA	84.0	28.3	25,007	1,405	-42.0
No origin seen on MRA	96.8	38.7	40,362	2,235	-51.0
Reduction	-13.2%	-27.0%	-38.0%	-37.1%	-17.7%
<i>p</i>	0.25	0.028	0.003	0.003	0.54

DAP, dose area product; IPSS, international prostate symptom score; PA, prostatic artery; MRA, magnetic resonance angiography.

Table 6. Changes in all baseline values before and after prostatic artery embolization in a cohort of 33 patients that completed clinical and imaging follow-up

	Pre-embolization n=33	Post-embolization n=33	Change	Percent change	<i>p</i>
IPSS	21.00 \pm 6.91 (11 to 35)	11.33 \pm 8.04 (2 to 3)	-9.67 \pm 8.21 (-30 to +8)	-45.58 \pm 31.88 (-88.0 to +30.0)	<0.001
QoL score	3.73 \pm 1.33 (0 to 6)	2.09 \pm 1.38 (0 to 6)	-1.63 \pm 1.45 (-4 to +2)	-41.70 \pm 36.36 (-100 to +50)	<0.001
IIEF score	17.45 \pm 10.09 (1 to 30)	20.33 \pm 9.72 (1 to 30)	+2.88 \pm 6.14 (-8 to +26)	103.39 \pm 453.41 (-35 to +2600)	0.004
PV (mL)	74.17 \pm 33.08 (35.33 to 171.48)	67.26 \pm 31.58 (25.64 to 161.77)	-6.91 \pm 9.46 (-38.15 to +7.47)	-9.03 \pm 12.96 (-50.1 to +7.7)	<0.001

Data are presented as mean \pm SD (min-max).

A decrease in IPSS and QoL means clinical improvement, whereas an increase in IIEF means an improvement in erectile function.

IPSS, international prostate symptom score (possible range, 0-35); SD, standard deviation; QoL, quality of life score (possible range, 0-6); IIEF, international index of erectile function (possible range, 1-30); PV, prostate volume.

clinical outcome, radiation parameters or procedure time were given. Patients with technical suboptimal MRA were excluded from the study and there was only a spatial resolution of matrix 256×179. Besides these differences, same amount and type of contrast media was used as in our study.

Zhang et al. (4) conducted a randomized prospective trial with 100 patients. In total, 91.5% of the PAs could be seen in MRA analysis prior to PAE (4). All the stated PA origins were later confirmed via DSA. Zhang et al. (4) documented a significant reduction in procedure time (33.6%), fluoroscopy time (51.6%), DAP (35.5%), and entrance dose (63.2%). The documented DAP suits the findings of this study as well as the 75% reduction of IPSS. However, the injection rate of 3 mL/s and higher amount of contrast media applied with a power injector as well as the retrospective setting could be responsible for the better accuracy detected. Mean baseline parameters of this cohort differ from our patients as the patients of Zhang et al. (4) were on average 4 years older and had about 25 mL larger prostates as well as approximately 3 points higher IPSS.

Successful 3D reconstruction of contrast-enhanced MRA is not only useful for analyzing PA origin but for predicting the best tube angle obliquity for the C-arm CT during PAE. Both previous studies used MIP, multiplanar reformation and curved planar reformation for MRA reconstruction and origin analysis. The obtained 3D volume-rendered model reconstruction has the advantage of offering maximal flexibility in rotation contrary to rotational maximum intensity projections which has fixed angles in one direction (17).

CTA is not performed regularly at our institute prior to PAE due to the additional radiation and contrast media exposure. Instead every patient undergoes a multiparametric MRI prior to such interventions to observe detailed morphologic and volumetric information and rule out possible signs of malignancy. Furthermore, MRI allows detailed assessment of parenchyma and is the most appropriate technique for analysis of PV and other morphologic features as intravesical prostatic protrusion or prostatic urethral angle (13, 18, 19).

The reduction of radiation by performing MRA ahead of angiographic procedures was previously investigated by Naguib et al. (17) regarding uterine artery embolization as well as by Zhang et al. (4) regarding the

PAE procedure. Both studies describe significant reduction of radiation dose due to 3D vessel reconstruction up to 62%.

As PAE is a complicated procedure, high radiation exposure needs to be expected. In previous literature, there is one case described with direct radiation damages in form of radiodermatitis with a DAP of 8,023,949 mGy·cm², whereas others describe a DAP of 450.7 Gy·cm² and a peak skin dose of 2420.3 mGy (20, 21).

Effectiveness of MRA-planned PAE was demonstrated with clinical outcome showing a highly significant improvement of -9.67 (-45.58%) in IPSS and clinical success rate of 72.7%. These findings are comparable to results of CTA-planned and prospective PAE studies, which reached clinical success rates about 78% at 6 months follow-up and a decrease of IPSS of 44.8 % and reinforce eligibility of MRA-planned PAE as an approved method (5, 12, 22).

A similar study by Zhang et al. (4) emphasized the importance of MRA prior to PAE. The current study agrees with their findings. However, there are some differences between the two studies. While Zhang et al. (4) used rotational MIP at 5° fixed interval our 3D volume-rendered model offers much more flexibility which is sometimes important to clearly visualize the origin of the PA or identify it and trace it back to its origin. The main advantage here is that with our technique we could make fine adjustment to the angle including adjustments in 1° intervals and not only in the side-to-side direction as in the study of Zhang et al. (4) but also in the craniocaudal direction which is sometimes required to project the PA away from the other arteries to clearly see its origin.

Our findings concerning positive effects on IIEF score match those in the literature, which described these effects as an important advantage of PAE over other therapies and suggested suitability of PAE especially for younger, sexually active patients as well as for highly comorbid patients who are not suitable for anesthesia (5, 8, 19, 23–26).

Limitations of this single-center study comprise the small sample size and retrospective nature of this study. Furthermore, only the origin of PA was analyzed and no precise analysis of the intraprostatic distribution pattern was documented. Further prospective randomized studies comparing the performance of MRA and CTA before PAE are required as well as studies to examine if MRA quality and sensitivity

can be further optimized, e.g., if the usage of a vasodilator can improve MRA quality. Another issue is the possible difference in diameter of the prostatic artery which might lead to failed identification on MRA. However, owing to the very small range of the PA in diameter and the difficulty to measure this diameter accurately, especially since the diameter might vary along the length of the artery, this was not performed in the current study. Still, we think the continuous development of the technology might solve the problem of the resolution and allow an accurate measure of the diameter of such small structures in the future.

In conclusion, MRA may facilitate preparation for the PAE procedure and provide guidance during angiography. It is an important and effective radiation-free pre-interventional method to plan PAE. It shows an equally good clinical outcome compared with other imaging methods and therefore might be suitable for analyzing PA origin prior to PAE.

Conflict of interest disclosure

The authors declared no conflicts of interest.

References

1. Bilhim T, Tinto HR, Fernandes L, Martins Pisco J. Radiological anatomy of prostatic arteries. *Tech Vasc Interv Radiol* 2012; 15:276–285. [\[Crossref\]](#)
2. Assis AM de, Moreira AM, Paula Rodrigues VC de, et al. Pelvic arterial anatomy relevant to prostatic artery embolisation and proposal for angiographic classification. *Cardiovasc Intervent Radiol* 2015; 38:855–861. [\[Crossref\]](#)
3. Maclean D, Maher B, Harris M, et al. Planning prostate artery embolisation: is it essential to perform a pre-procedural CTA? *Cardiovasc Intervent Radiol* 2018; 41:628–632.
4. Zhang JL, Wang MQ, Shen YG, et al. Effectiveness of contrast-enhanced MR angiography for visualization of the prostatic artery prior to prostatic arterial embolization. *Radiology* 2019; 291:370–378. [\[Crossref\]](#)
5. Pisco JM, Rio Tinto H, Campos Pinheiro L, et al. Embolisation of prostatic arteries as treatment of moderate to severe lower urinary symptoms (LUTS) secondary to benign hyperplasia: Results of short- and mid-term follow-up. *Eur Radiol* 2013; 23:2561–2572. [\[Crossref\]](#)
6. Carnevale FC, Soares GR, Assis AM de, Moreira AM, Harward SH, Cerri GG. Anatomical variants in prostate artery embolization: a pictorial essay. *Cardiovasc Intervent Radiol* 2017; 40:1321–1337. [\[Crossref\]](#)
7. Hacking N, Vigneswaran G, Maclean D, et al. Technical and imaging outcomes from the UK registry of prostate artery embolization (UK-ROPE) study: focusing on predictors of clinical success. *Cardiovasc Intervent Radiol* 2019; 42:666–676. [\[Crossref\]](#)

8. Carnevale FC, Iscaife A, Yoshinaga EM, Moreira AM, Antunes AA, Srougi M. Transurethral resection of the prostate (TURP) versus original and PErFecTED prostate artery embolization (PAE) due to benign prostatic hyperplasia (BPH): preliminary results of a single center, prospective, urodynamic-controlled analysis. *Cardiovasc Intervent Radiol* 2016; 39:44–52. [\[Crossref\]](#)
9. Wang M, Guo L, Duan F, et al. Prostatic arterial embolization for the treatment of lower urinary tract symptoms caused by benign prostatic hyperplasia: A comparative study of medium- and large-volume prostates. *BJU Int* 2016; 117:155–164. [\[Crossref\]](#)
10. Wang MQ, Duan F, Yuan K, Zhang GD, Yan J, Wang Y. Benign prostatic hyperplasia: cone-beam CT in conjunction with DSA for identifying prostatic arterial anatomy. *Radiology* 2017; 282:271–280. [\[Crossref\]](#)
11. DeMeritt JS, Wajswol E, Wattamwar A, Osiason A, Chervoni-Knapp T, Zamudio S. Duplicated prostate artery central gland blood supply: a retrospective analysis and classification system. *J Vasc Interv Radiol* 2018; 29:1595–1600. [\[Crossref\]](#)
12. Pisco J, Campos Pinheiro L, Bilhim T, et al. Prostatic arterial embolization for benign prostatic hyperplasia: Short- and intermediate-term results. *Radiology* 2013; 266:668–677. [\[Crossref\]](#)
13. Kim AY, Field DH, DeMulder D, Spies J, Krishnan P. Utility of MR angiography in the identification of prostatic artery origin prior to prostatic artery embolization. *J Vasc Interv Radiol* 2018; 29:307–310.e1.
14. Prince MR. MR angiography of the prostate arteries: benefit prior to prostate embolization. *Radiology* 2019; 291:379–380. [\[Crossref\]](#)
15. Maclean D, Harris M, Drake T, et al. Factors predicting a good symptomatic outcome after prostate artery embolisation (PAE). *Cardiovasc Intervent Radiol* 2018; 41:1152–1159. [\[Crossref\]](#)
16. Du Pisanie J, Aboumoussa A, Donovan K, Stewart J, Bagla S, Isaacson A. Predictors of prostatic artery embolization technical outcomes: patient and procedural factors. *J Vasc Interv Radiol* 2019; 30:233–240. [\[Crossref\]](#)
17. Naguib NNN, Nour-Eldin N-EA, Lehnert T, et al. Uterine artery embolization: Optimization with preprocedural prediction of the best tube angle obliquity by using 3D-reconstructed contrast-enhanced MR angiography. *Radiology* 2009; 251:788–795. [\[Crossref\]](#)
18. Andrade G, Khoury HJ, Garzón WJ, et al. Radiation exposure of patients and interventional radiologists during prostatic artery embolization: a prospective single-operator study. *J Vasc Interv Radiol* 2017; 28:517–521. [\[Crossref\]](#)
19. Laborda A, Assis AM de, Ioakeim I, Sánchez-Ballestín M, Carnevale FC, Gregorio MA de. Radiodermatitis after prostatic artery embolization: Case report and review of the literature. *Cardiovasc Intervent Radiol* 2015; 38:755–759. [\[Crossref\]](#)
20. Bilhim T, Pisco J, Rio Tinto H, et al. Unilateral versus bilateral prostatic arterial embolization for lower urinary tract symptoms in patients with prostate enlargement. *Cardiovasc Intervent Radiol* 2013; 36:403–411. [\[Crossref\]](#)
21. Zhang H, Shen Y, Pan J, et al. MRI features after prostatic artery embolization for the treatment of medium- and large-volume benign hyperplasia. *Radiol Med* 2018; 123:727–734. [\[Crossref\]](#)
22. Carnevale FC, Antunes AA. Prostatic artery embolization for enlarged prostates due to benign prostatic hyperplasia. How I do it. *Cardiovasc Intervent Radiol* 2013; 36:1452–1463.
23. Wang X-Y, Zong H-T, Zhang Y. Efficacy and safety of prostate artery embolization on lower urinary tract symptoms related to benign prostatic hyperplasia: A systematic review and meta-analysis. *Clin Interv Aging* 2016; 11:1609–1622. [\[Crossref\]](#)
24. Malling B, Röder MA, Brasso K, Forman J, Taudorf M, Lönn L. Prostate artery embolisation for benign prostatic hyperplasia: A systematic review and meta-analysis. *Eur Radiol* 2019; 29:287–298. [\[Crossref\]](#)
25. Shim SR, Kanhai KJK, Ko YM, Kim JH. Efficacy and safety of prostatic arterial embolization: systematic review with meta-analysis and meta-regression. *J Urol* 2017; 197:465–479. [\[Crossref\]](#)
26. McWilliams JP, Bilhim TA, Carnevale FC, et al. Society of Interventional Radiology Multisociety Consensus Position Statement on Prostatic Artery Embolization for Treatment of Lower Urinary Tract Symptoms Attributed to Benign Prostatic Hyperplasia: From the Society of Interventional Radiology, the Cardiovascular and Interventional Radiological Society of Europe, Société Française de Radiologie, and the British Society of Interventional Radiology: Endorsed by the Asia Pacific Society of Cardiovascular and Interventional Radiology, Canadian Association for Interventional Radiology, Chinese College of Interventionalists, Interventional Radiology Society of Australasia, Japanese Society of Interventional Radiology, and Korean Society of Interventional Radiology. *J Vasc Interv Radiol* 2019; 30:627–637. [\[Crossref\]](#)